

Alma Mater Studiorum Università di Bologna
Archivio istituzionale della ricerca

Spectroscopy of a low global warming power refrigerant. Infrared and millimeter-wave spectra of trifluoroethene (HFO-1123) in the ground and some vibrational excited states

This is the final peer-reviewed author's accepted manuscript (postprint) of the following publication:

Published Version:

Tamassia F., Melosso M., Dore L., Pettini M., Cane' E., Stoppa P., et al. (2020). Spectroscopy of a low global warming power refrigerant. Infrared and millimeter-wave spectra of trifluoroethene (HFO-1123) in the ground and some vibrational excited states. JOURNAL OF QUANTITATIVE SPECTROSCOPY & RADIATIVE TRANSFER, 248, 1-7 [10.1016/j.jqsrt.2020.106980].

Availability:

This version is available at: <https://hdl.handle.net/11585/778702> since: 2021-02-17

Published:

DOI: <http://doi.org/10.1016/j.jqsrt.2020.106980>

Terms of use:

Some rights reserved. The terms and conditions for the reuse of this version of the manuscript are specified in the publishing policy. For all terms of use and more information see the publisher's website.

This item was downloaded from IRIS Università di Bologna (<https://cris.unibo.it/>).
When citing, please refer to the published version.

(Article begins on next page)

This is the final peer-reviewed accepted manuscript of:

Filippo Tamassia, Mattia Melosso, Luca Dore, Michele Pettini, Elisabetta Canè, Paolo Stoppa, Andrea Pietropolli Charmet, "Spectroscopy of a low global warming power refrigerant. Infrared and millimeter-wave spectra of trifluoroethene (HFO-1123) in the ground and some vibrational excited states," *Journal of Quantitative Spectroscopy and Radiative Transfer*, 248, 106980 (2020)

The final published version is available online at:

<https://doi.org/10.1016/j.jqsrt.2020.106980>

Terms of use:

Some rights reserved. The terms and conditions for the reuse of this version of the manuscript are specified in the publishing policy. For all terms of use and more information see the publisher's website.

This item was downloaded from IRIS Università di Bologna
(<https://cris.unibo.it/>)

When citing, please refer to the published version.

Spectroscopy of a Low Global Warming Power Refrigerant. Infrared and Millimeter-wave Spectra of Trifluoroethene (HFO-1123) in the Ground and some Vibrational Excited States

Filippo Tamassia^{a,*}, Mattia Melosso^b, Luca Dore^b, Michele Pettini^b, Elisabetta Canè^a, Paolo Stoppa^c,
Andrea Pietropolli Charmet^{c,*}

^a*Dipartimento di Chimica Industriale “Toso Montanari”, Università di Bologna, Viale del Risorgimento 4, 40136 Bologna (Italy)*

^b*Dipartimento di Chimica “Giacomo Ciamician”, Università di Bologna, Via F. Selmi 2, 40126 Bologna (Italy)*

^c*Dipartimento di Scienze Molecolari e Nanosistemi, Università Ca’ Foscari Venezia, Via Torino 155, 30172 Mestre (Italy)*

Abstract

In the present work we carried out a combined rotational and ro-vibrational investigation on 1,1,2-trifluoroethene, a relevant unsaturated hydrofluoroolefin recently proposed as refrigerant in mixture with other halogenated compounds (like difluoromethane). By employing a frequency-modulation millimeter-wave spectrometer, the rotational spectra were recorded in the frequency ranges 80–96 GHz and 245–260 GHz for the ground and also the vibrationally excited states $\nu_8 = 1$, $\nu_9 = 1$, $\nu_{12} = 1$, $\nu_9 = 2$, $\nu_{12} = 2$, and $\nu_9 = \nu_{12} = 1$. In addition, the infrared spectra in the region of the ν_6 band (centered at 929.8 cm^{-1}) were measured with a high-resolution Fourier transform spectrometer. The data coming from the detailed rotational and ro-vibrational assignments were combined in a global fit, taking into account also the ground state transitions available in the literature. From this analysis, a very accurate set of rotational and centrifugal distortion constants was determined for the ground state and for all the vibrationally excited states here investigated.

Keywords: Rotational Spectroscopy, Ro-vibrational spectra, Hydrofluoroolefins, Trifluoroethene, HFO-1123

1. Introduction

In the last decades, great attention has been devoted to the search for suitable replacements of the gases used for domestic and industrial purposes which strongly contribute to the atmospheric pollution, the ozone hole and the greenhouse effect. Unsaturated hydrofluoroolefins (HFO’s) are an interesting alternative to chlorofluorocarbons (CFC’s). Indeed, such molecules have a very short atmospheric lifetime, an almost zero Ozone Depletion Potential (ODP) and a low Global Warming Potential (GWP) [1]. The search of an ideal candidate for refrigerants is nowadays a crucial issue, considering that recent studies showed that a very limited number of fluids exhibit the required environmental properties [2]. 1,1,2-trifluoroethene ($\text{CF}_2=\text{CHF}$, HFO-1123, hereafter referred as TFE) is used nowadays in heat pumps and conditioning systems, often in mixtures with difluoromethane (CH_2F_2 , HFC-32). In these mixtures self-decomposition does not occur [1]; also, they have low toxicity and are only mildly flammable [1, 3], proving therefore to be a valuable alternative to R-410A, a common refrigerant with high GWP. The atmospheric importance of $\text{CF}_2=\text{CHF}$ has stimulated a number of spectroscopic studies in the past. Low resolution infrared (IR) spectra were first recorded by Mann *et al.* [4] and later by McKean [5]. In 2002

*Corresponding author

Email addresses: filippo.tamassia@unibo.it (Filippo Tamassia), jacpnike@unive.it (Andrea Pietropolli Charmet)

Jiang *et al.* [6] calculated the vibrational fundamental wavenumbers and the relative intensities using the Scaled Quantum Mechanical (SQM) force field procedure in combination with the hybrid three-parameter B3-PW91 density functional. Microwave transitions of the ground and some vibrationally excited states were reported a long time ago by Bhaumik *et al.* [7] and Wellington Davis & Gerry [8].

More recently, Leung & Marshall recorded rotational transitions of TFE between 6 and 22 GHz by Fourier transform (FT) spectroscopy for the most abundant isotopologue and the two singly ^{13}C -substituted species. From the determined spectroscopic constants they also derived the structural parameters of the molecule [9]. High-resolution infrared studies are however limited to the very strong fundamentals ν_3 , ν_4 , and ν_5 in the atmospheric window, centered at 1360, 1265, and 1173 cm^{-1} , respectively. These high-resolution spectra were recorded with a tunable diode laser and analysed by Visinoni *et al.* [10, 11, 12]. The authors pointed out the presence of several resonances and determined some parameters for the interacting states.

The infrared atmospheric window has been only partially analysed and this work aims to a more complete spectroscopic characterization of this region and of the low-lying vibrational states. The goal is to provide the necessary laboratory data useful for the atmospheric detection of this molecule. The infrared spectrum was recorded at high resolution (0.004 cm^{-1}) by FT-IR spectroscopy between 500 and 1500 cm^{-1} , where the ν_3 , ν_4 , ν_5 , ν_6 (929 cm^{-1}), ν_7 (623 cm^{-1}) and ν_{10} (750 cm^{-1}) fundamental bands are located with the objective to assign and analyse for the first time ν_6 , ν_7 , and ν_{10} and to re-investigate ν_3 , ν_4 , and ν_5 . Given the complexity of the ro-vibrational structure, in this paper we focused only on the ν_6 fundamental vibrational band and on the detection of pure rotational transitions in the ground state and in the low energy $v_8 = 1$, $v_9 = 1$, $v_{12} = 1$, $v_9 = 2$, $v_{12} = 2$, and $v_9 = v_{12} = 1$ excited vibrational states. The rotational spectra were recorded in the frequency ranges 80-96 GHz and 245-260 GHz using a frequency-modulation millimeter-wave spectrometer.

In this work we present therefore a combined rotational and ro-vibrational investigation from which very accurate spectroscopic parameters were determined for the ground state and the investigated excited vibrational states.

2. Experimental details

2.1. Millimeter spectrometer

Rotational spectra were recorded in the frequency ranges 80-96 GHz and 245-260 GHz using a frequency-modulation millimeter-wave spectrometer [13, 14]. The radiation source is a Gunn diode (J.E. Carlstrom Co.) emitting in the spectral range 80-115 GHz with an output power up to 50 mW. A passive multiplier (WR3.4X2, Virginia Diodes) is used to reach the higher frequencies. The diode's radiation is phase-locked to a harmonic of a digital frequency synthesizer (HP8672A, 2-18 GHz) and its frequency is sine-wave modulated by a 75 MHz reference signal. Each synthesizer is referenced to a rubidium atomic-clock which guarantees the frequency stability of the radiation. A 3.25 m-long free-space glass absorption cell, filled with trifluoroethene vapor at a static pressure between 1 and 2.5 Pa, was employed for the measurements. The output signal was sensed by two different zero-biased Schottky diode detectors (Millitech, Inc. below 100 GHz and Virginia Diodes above 240 GHz) and demodulated at twice the modulation frequency by an analog lock-in amplifier. The signal is then filtered into an ohmic RC circuit, analog-to-digital converted and sent to a computer. Typically, the spectra were recorded using a frequency modulation $f = 48$ kHz, a modulation depth (FM) between 90 and 300 kHz, a RC constant of 3 ms, and a frequency step sufficiently small to provide at least twenty points across the expected linewidths.

2.2. Infrared spectra

The vibrational spectra were recorded with a FT-IR Bomem spectrometer [15], equipped with an MCT detector and a Globar source. The resolution of the spectra was 0.004 cm^{-1} and the optical pathlength, obtained with a multipass absorption cell, was 3 meters. Sample pressures ranged between 0.06 and 1 hPa. Several hundreds scans were co-added in order to improve the signal-to-noise ratio of the spectra. The absolute calibration of the wavenumber axis was attained by referencing ro-vibrational transitions of H_2O and CO_2 from the HITRAN database [16]. An overview of the high-resolution infrared spectrum between 500 and 1500 cm^{-1} is shown in Figure 1.

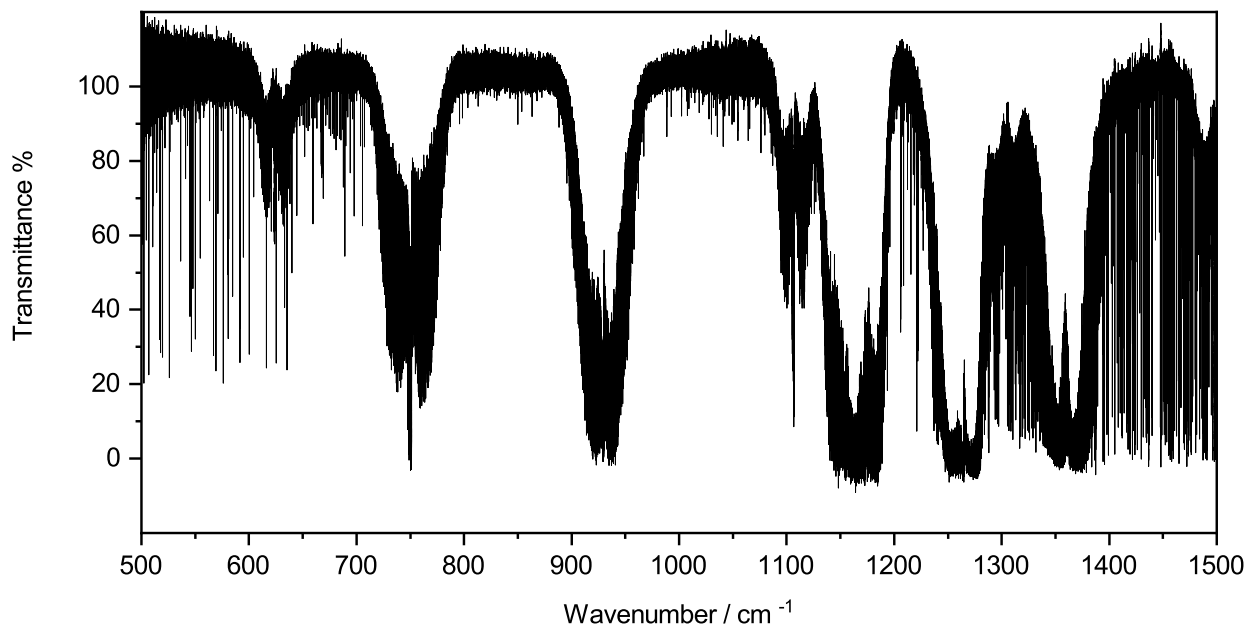


Figure 1: Portion of the infrared spectrum ($P=1$ hPa, $L=3$ m, 800 scans, room temperature). The assignment of all fundamental bands is given in Table 1.

3. Analysis and results

3.1. General features

From a spectroscopic point of view, trifluoroethene is a planar near-prolate asymmetric-top molecule belonging to the C_s symmetry point group, having an asymmetry parameter $\kappa=-0.74$. The molecular geometry of TFE with respect to its principal axes is shown in Figure 2.

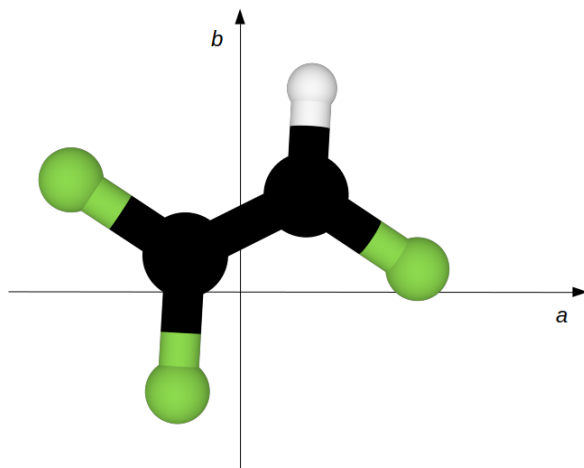


Figure 2: Trifluoroethene in its principal axis system.

Its permanent electric dipole moment ($\mu=1.30(6)$ D) lies in the ab plane, with the b component ($\mu_b=1.30(6)$ D) much greater than that of the a component ($\mu_a=0.075(15)$ D) [7]. Of the 12 fundamentals, all infrared active, 9 are classified as A' modes ($\nu_1 - \nu_9$), whereas the other 3 are A'' ($\nu_{10} - \nu_{12}$). The former give rise to a/b

hybrid bands, while the latter produce *c*-type band contours. The vibrational modes and their description are summarized in Table 1.

Table 1: Vibrational modes.

Symmetry	Mode	Envelope	Rel. intensity ^a	Description	Wavenumber ^b	Reference
A'	ν_1	a/b	m	C–H stretch.	3150	[4]
	ν_2		s	C=C stretch.	1788	[4]
	ν_3		vs	CF ₂ antisym. stretch.	1361.3684(1)	[10]
	ν_4		vs	C–F stretch.	1264.86188(4)	[11]
	ν_5		vs	CHF bend.	1172.6730(1)	[12]
	ν_6		s	CF ₂ sym. stretch.	928.80082(6)	This work
	ν_7		m	C–F bend.	623	[4]
	ν_8		w	CF ₂ bend.	485	[4]
	ν_9		w	CF ₂ rock.	232	[4]
A''	ν_{10}	c	s	CHF oop bend.	750	[4]
	ν_{11}		vw	CF ₂ wag.	555	[4]
	ν_{12}		w	Torsion	305	[4]

^a Abbreviations are used as follows: vs = very strong, s = strong, m = medium, w = weak, vw = very weak.

^b Units are cm^{−1}. Numbers in parenthesis represent quoted uncertainties.

The ro-vibrational energies have been modeled by the standard semi-rigid Watson’s *A*-reduced Hamiltonian [17] in the *I*^r representation:

$$\mathcal{H} = \mathcal{H}_{\text{vr}} + \mathcal{H}_{\text{cd}}^{(4)} + \mathcal{H}_{\text{cd}}^{(6)} + \dots, \quad (1)$$

where \mathcal{H}_{vr} contains the vibrational energy E_v and the rotational constants A , B , and C :

$$\mathcal{H}_{\text{vr}} = E_v + \frac{1}{2} (B + C) \mathbf{P}^2 + \left[A - \frac{1}{2} (B + C) \right] \mathbf{P}_a^2 + \frac{1}{2} (B - C) (\mathbf{P}_b^2 - \mathbf{P}_c^2). \quad (2)$$

\mathbf{P} is the operator of the total angular momentum and \mathbf{P}_a , \mathbf{P}_b , and \mathbf{P}_c its components along the principal inertial axes in the molecule-fixed coordinate system. The $\mathcal{H}_{\text{cd}}^{(4)}$ part accounts for the centrifugal distortion terms up to 4th power of the angular momentum

$$\mathcal{H}_{\text{cd}}^{(4)} = -\Delta_J \mathbf{P}^4 - \Delta_{JK} \mathbf{P}^2 \mathbf{P}_a^2 - \Delta_K \mathbf{P}_a^4 - \delta_J \mathbf{P}^2 (\mathbf{P}_b^2 - \mathbf{P}_c^2) - \delta_K [\mathbf{P}^2 (\mathbf{P}_b^2 - \mathbf{P}_c^2) + (\mathbf{P}_b^2 - \mathbf{P}_c^2) \mathbf{P}^2], \quad (3)$$

while $\mathcal{H}_{\text{cd}}^{(6)}$ contains operator with 6th power of \mathbf{P} [see Ref. 18, Eq. (8.100)], and so on. For the ground state only the analysis has also been performed in the Watson’s *S*-reduced Hamiltonian [17]. Its form is not reported here and can be found in Ref. [18], Eqs. (8.110)–(8.113).

Since hydrogen and fluorine possess a non-vanishing nuclear spin ($I = 1/2$), rotational energy levels can exhibit a hyperfine-structure due to nuclear spin-spin interactions. These effects were observed for few transitions recorded with a pulsed Fourier-transform microwave spectrometer [9], but they are too small to be detected at high frequencies or in infrared spectra.

3.2. Rotational spectra

Initially, the rotational spectrum of TFE in its ground vibrational state has been predicted using the spectroscopic constants reported in Ref. [8]. Literature data were limited to rotational transitions recorded at

frequencies below 66 GHz, corresponding to energy levels with J up to 75. Therefore, the available set of spectroscopic parameters (rotational constants and centrifugal distortion terms) provided reliable predictions in our spectral coverage.

In the 80–96 GHz window, rotational transitions have been recorded mostly line-by-line, scanning few MHz around the predicted transition frequencies. On the other hand, in the 245–260 GHz range, where the lines are more spread out, scanning broader portions was more convenient (see Figure 3).

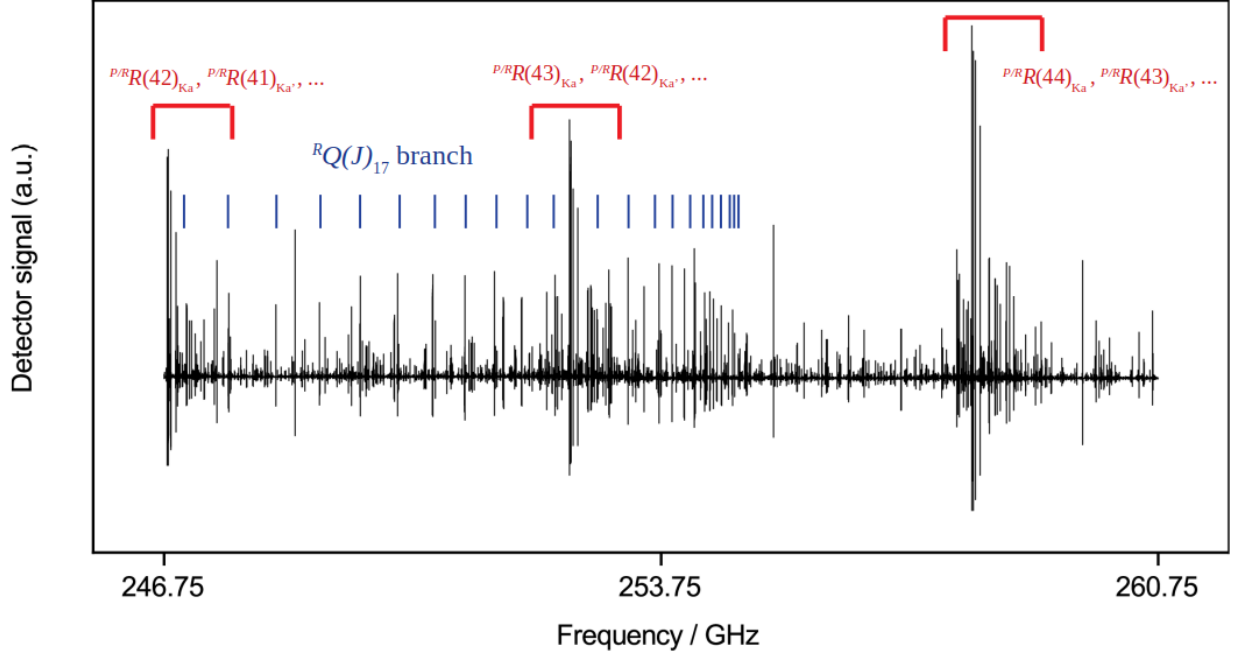


Figure 3: Portion of the millimeter spectrum of trifluoroethene. The spectrum has been obtained by adding consecutive 250 MHz-long scans, all of which were recorded sweeping the frequency upward and downward for an integration time of *ca.* 200 s. The figure shows the complexity of the rotational spectrum, where some $P/R R(J)_{K_a}$ transitions are grouped at certain frequencies. Also, the $RQ(J)_{17}$ branch is reported.

A number of 260 b -type transition frequencies have been recorded and added to the previous data set [7, 8, 9], expanding the data up to $J = 106$ and requiring the inclusion of higher order centrifugal distortion terms. Singly excited states ($\nu_8 = 1$, $\nu_9 = 1$, and $\nu_{12} = 1$) transitions up to 96 GHz were predicted by using the spectroscopic constants of Refs. [7, 8]. More precise spectral predictions were later produced in order to assign the broad spectrum between 245 and 260 GHz. The transitions relative to the doubly excited vibrational states ($\nu_9 = 2$, $\nu_{12} = 2$, and $\nu_9 = \nu_{12} = 1$) were initially calculated with rotational parameters derived from the rotational constants of the corresponding singly excited vibrational states and the derived ro-vibrational coupling constants α . Although the $\nu_{11} = 1$ state is lower in energy than the $\nu_{12} = 2$ and its rotational lines should be detected more easily because of the higher Boltzmann population, it was not possible to confidently assign any transitions of the $\nu_{11} = 1$ state. Indeed, the density of lines in the spectrum and the lack of reliable predictions for the $\nu_{11} = 1$ state made the assignment of transitions belonging to this excited vibrational state very difficult. On the other hand, it was easier to recognize transitions of $\nu_{12} = 2$, despite its higher vibrational energy, because the knowledge of the α constants derived from the singly excited $\nu_{12} = 1$ state allowed rather precise predictions.

3.3. The ν_6 fundamental band

The structure of the Q branch of the ν_6 fundamental, degrading to lower wavenumbers, appears very dense and the even ($K_a'' + K_c'' = J''$) and odd ($K_a'' + K_c'' = J'' + 1$) transitions are mostly overlapped. Anyway, the

high-wavenumber edge of the Q branch allowed us to estimate the band origin; this datum, combined with the ground state constants, led to the identification near the band center of several ${}^Q P_K(J)$ and ${}^Q R_K(J)$ groups, which are approximately separated by $(B + C) \simeq 0.22 \text{ cm}^{-1}$. As the J values increase, the lines belonging to a given cluster start to overlap to a great extent with those of the neighboring manifolds, thus leading to a very packed structure where the resolved details are very difficult to identify. The most relevant information for the analysis of the band was yielded by the assignment of groups of lines having high J and low K_a values. In both the P and R branches, the spectrum is dominated by distinct bandheads; they are separated by about $2C \simeq 0.18 \text{ cm}^{-1}$ and consist of a series of transitions having the J values differing by one unit between successive lines, each one involving the levels with K_a^+ and $(K_a + 1)^-$, which are almost degenerate (the superscripts + and - refer to even and odd transitions, respectively). These spectral features are characteristic of planar molecules; Borchert[19] and Kisiel[20] are the first who investigated these patterns highlighting that they are due to the near-coincidence of transitions between energy levels which become degenerate in the oblate symmetric top limit. Figure 4 reproduces a section of the R branch near 940.3 cm^{-1} with the resolved J lines in the ${}^Q R_K(J = 50 - 59)$ bandheads. The series starts with the transition having $J'' = K_c''$, and then proceeds toward the higher frequency side with the line sequences of the two degenerate even and odd components given, in the R branch, by

$$(J - k + 1)_{k, J-2k+1} \leftarrow (J - k)_{k, J-2k} \quad (4)$$

$$(J - k + 1)_{k+1, J-2k+1} \leftarrow (J - k)_{k+1, J-2k} \quad (5)$$

where $k = 0, 1, 2, 3, \dots$

By using the constants derived from the analysis of the a -type component we tried to identify also the b -type transitions, but they could not be reliably assigned given their lower intensities and the very packed structure of the spectrum.

4. Discussion

The fitting procedure, the spectral simulation and the calculation of the ro-vibrational term values were carried out by employing the ATIRS software [21] and the SPFIT/SPCAT program suite [22]. The rotational and ro-vibrational data were analysed in a global fit together with the literature data for the ground state only [7, 8, 9]. The transition frequencies of Ref. [7] relative to vibrationally excited states were not used in our global fit, not only because they are less precise than our measurements, but also because they show residuals much greater than the stated uncertainties.

In Tables 2– 4 the spectroscopic parameters determined for the ground and vibrationally excited states are reported. Although the global fit was performed using the Watson A -reduced Hamiltonian, in the case of the ground state (Table 2), the fits have been performed in both the A and S reductions and are compared with the literature results of Ref. [8]. The quality of the two procedures is equivalent, in terms of root-mean-square (RMS) error and standard deviation σ , but the precision of the individual parameters is greatly improved in both cases, with respect to previous determination [8, 9]. This is consistent with the much wider range of J and K_a values observed in this work, which allowed precise derivations even for high-order centrifugal distortion terms. As can be seen from inspection of Table 2, our rotational constants (A , B , C) as well as our set of quartic centrifugal distortion terms agree well with those reported in the literature [8, 9]. On the other hand, the values of all the sextic centrifugal constants are totally different from those of Ref. [8] because (i) our analysis includes a more various sample of transitions and (ii) most of the sextic constants were completely undetermined in Ref. [8] (i.e., the uncertainty on the constants were greater than the constants themselves).

In Table 3 the results for the singly excited vibrational states $\nu_9 = 1$, $\nu_{12} = 1$, $\nu_8 = 1$ and $\nu_6 = 1$ are presented. As discussed previously, only the ν_6 fundamental ro-vibrational band has been analysed, while pure rotational transitions were observed for the other vibrational states.

For the fundamental ν_6 , the analysis carried out in the P and R branches led to the assignment of many transitions (belonging to the a -type component) having $J \leq 85$ and $K_a \leq 11$. Only well resolved features

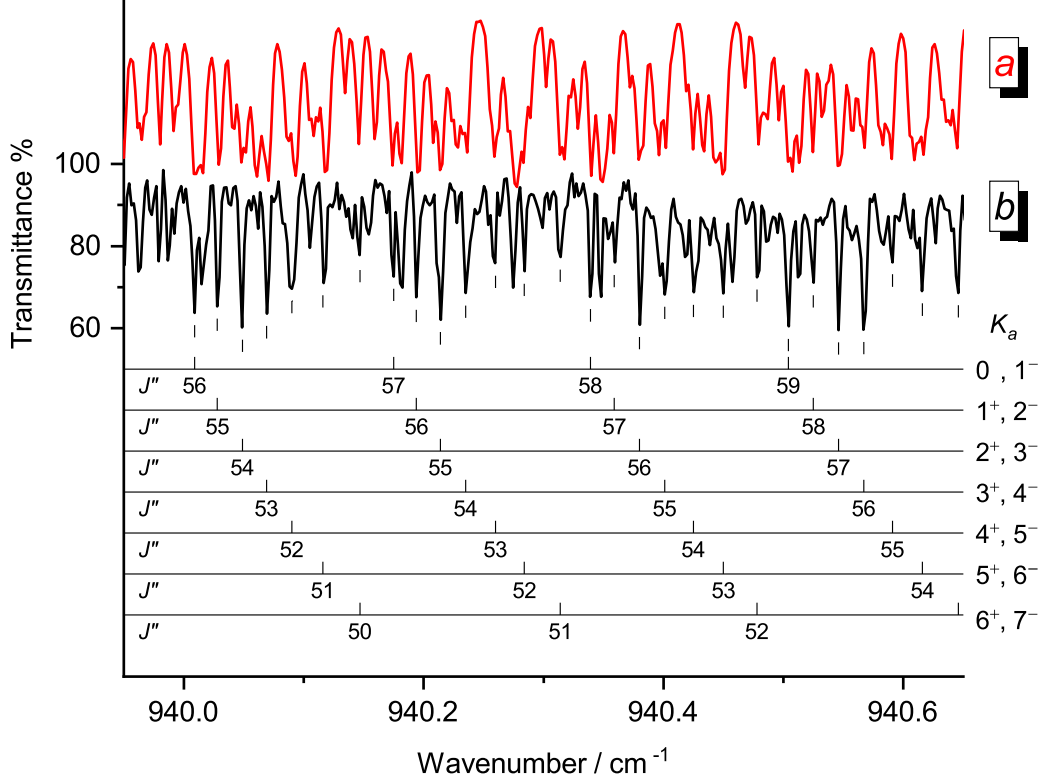


Figure 4: Details of the FT-IR spectrum of the ν_6 band around 940.3 cm^{-1} . Lower (black) trace *b* refers to the experimental spectrum, upper (red) trace *a* refers to the computed one using our best parameters. The line sequences in the $Q_{R_K}(J'' = 50 - 59)$ band heads are reported.

were included in the analysis, while badly overlapped features were not considered. It is worthwhile to point out that the ro-vibrational assignments in the *P* and *R* branches were checked out by ground state combination differences (GSCDs) as implemented in the Visual Loomis Wood program (a part of the ATIRS package [21]). The RMS error shown from the final fit of 1622 ro-vibrational transitions is $7.5 \times 10^{-4} \text{ cm}^{-1}$. In addition to accurate values for band origin and rotational constants, all the quartic centrifugal distortion constants were refined in the fit, with the exception of Δ_K , due to the fact that K_a does not change in the observed transitions. The value of Δ_K was fixed to the ground state value. In addition, the sextic terms could not be reliably determined. It is useful to point out that the excited rotational and centrifugal distortion terms agree reasonably well with those of the ground state, thus confirming that the set of assigned transitions for the $\nu_6 = 1$ state is essentially free of perturbations. As a further check of the reliability of the results, spectral simulations were performed in different portions of the spectrum, as it can be seen by looking at Figure 4. The computed spectrum compares reasonably well with the experimental one (residual discrepancies are mainly due to signals coming from hot-bands and the weaker *b*-type component), thus pointing out the accuracy of the spectroscopic parameters here presented. Finally, Table 4 reports the parameters obtained from the analysis of the rotational transitions observed for the doubly excited vibrational states $\nu_9 = 2$, $\nu_{12} = 2$, and $\nu_9 = \nu_{12} = 1$. For these states, only a limited number of lines have been detected. Nevertheless, also in these cases precise sets of rotational and

Table 2: Spectroscopic parameters determined for trifluoroethene in the ground vibrational state.

Parameter ^[a]	Unit	Present work <i>A</i> -reduction	Previous ^[b]	Present work <i>S</i> -reduction	Previous ^[b]
A	MHz	10665.481287(51)	10665.47731(63)	10665.482129(54)	10665.47809(60)
B	MHz	3872.406579(24)	3872.40538(23)	3872.396511(26)	3872.39542(23)
C	MHz	2837.960953(29)	2837.95990(18)	2837.970162(31)	2837.96926(17)
$\Delta_J(D_J)$	kHz	0.731145(12)	0.73066(24)	0.560036(10)	0.56001(23)
$\Delta_{JK}(D_{JK})$	kHz	7.671250(62)	7.6757(29)	8.698079(51)	8.6985(23)
$\Delta_K(D_K)$	kHz	4.92912(16)	4.9248(15)	4.07290(17)	4.07168(66)
$\delta_J(d_1)$	kHz	0.1831457(50)	0.18353(16)	0.1831675(55)	−0.18346(18)
$\delta_K(d_2)$	kHz	4.83607(14)	4.8228(41)	0.0855201(26)	−0.085327(79)
$\Phi_J(H_J)$	mHz	0.2010(29)	0.038(20)	−0.0951(14)	0.056(89)
$\Phi_{JK}(H_{JK})$	Hz	0.019977(56)	0.0027(105)	0.005288(14)	0.0026(22)
$\Phi_{KJ}(H_{KJ})$	Hz	−0.05529(18)	0.0025(288)	−0.864(88)	0.0007(16)
$\Phi_K(H_K)$	Hz	0.07534(20)	0.033(21)	0.03395(17)	0.0306(27)
$\phi_J(h_1)$	mHz	0.0765(15)	−0.02(18)	0.0125(14)	−0.46(29)
$\phi_{JK}(h_2)$	mHz	9.352(55)	14.4(63)	0.1387(10)	0.59(25)
$\phi_K(h_3)$	Hz	0.11635(37)	−0.041(78)	0.07287(19)	0.00014(10)
$\Lambda_{JK}(L_{JK})$	nHz	−3.61(68)		23.05(71)	
Lines		484	182	484	182
$J_{\max}, K_{a\max}$		106, 38	75, 38	106, 38	75, 38
RMS error	kHz	21.6	16.0	21.6	15.8
σ		0.99	0.80	0.99	0.79

Notes: Numbers in parentheses are one standard deviation and apply to the last significant digits. **[a]** *S*-reduction parameters are reported in parentheses. **[b]** Ref. [8].

centrifugal distortion constants could be derived. The analysis of the rotational data in excited vibrational states highlighted the presence of accidental perturbations in all the states except $v_9 = 1$ and $v_{12} = 1$. A correct interpretation of perturbed transitions and their inclusion in the global analysis would require a detailed ro-vibrational analysis of the lowest excited states [23], not available at the moment. Therefore, only unperturbed transitions were included in the final analysis.

5. Conclusions

In this paper we report the detection of the rotational spectrum of TFE in the ground and in the vibrationally excited states $v_9 = 1$, $v_{12} = 1$, $v_8 = 1$, $v_9 = 2$, $v_{12} = 2$, and $v_9 = v_{12} = 1$. Moreover, the fundamental ν_6 ro-vibrational band has been observed. All the data were analysed in a global fit and sets of spectroscopic parameters for each state were determined in the *A*-reduction scheme. The quality of the fit is very good, as shown by the values of the statistical errors, the precision of the parameters and the overall good agreement between calculated and observed spectra. As far as the infrared bands are concerned, only a small portion of the recorded high-resolution spectrum has been analysed. In this light, this should be considered as an ongoing work.

We are already planning to study in the near future all the fundamentals not yet investigated, especially the ones falling below 500 cm^{-1} , for which a synchrotron-based experiment would be most appropriate.

Table 3: Spectroscopic parameters determined for trifluoroethene in the singly-excited vibrational states.

Parameter	Unit	$\nu_9 = 1$	$\nu_{12} = 1$	$\nu_8 = 1$	$\nu_6 = 1$
E	cm^{-1}	232 ^[a]	305 ^[a]	485 ^[a]	929.800817(68)
A	MHz	10624.33115(21)	10698.10053(46)	10673.4129(13)	10641.54(43)
B	MHz	3870.682459(76)	3879.11980(11)	3874.51307(24)	3867.839(43)
C	MHz	2835.673154(87)	2841.51433(10)	2835.73608(17)	2831.9027(19)
Δ_J	kHz	0.717141(44)	0.740172(89)	0.73194(26)	0.6934(89)
Δ_{JK}	kHz	6.72388(32)	8.33244(86)	7.6312(25)	8.66(23)
Δ_K	kHz	4.8686(22)	5.1612(33)	5.1076(32)	4.92907 ^[b]
δ_J	kHz	0.179378(16)	0.186624(31)	0.184212(84)	0.1656(44)
δ_K	kHz	4.38568(48)	5.22666(72)	4.8513(33)	5.049(44)
Φ_J	mHz	0.178(11)	0.223(26)	0.742(87)	
Φ_{JK}	mHz	4.18(24)	34.27(51)	26.16(59)	
Φ_{KJ}	Hz	−0.08034(91)	−0.0313(14)	−0.0220(47)	
Φ_K	Hz	0.0488(45)	0.0698(61)	0.07529 ^[b]	
ϕ_J	mHz	0.0308(56)	0.1015(99)	0.0768 ^[b]	
ϕ_{JK}	mHz	1.11(21)	17.02(34)	12.7(16)	
ϕ_K	Hz	0.0439(15)	0.1812(22)	0.11635 ^[b]	
Λ_{JKK}	μHz		0.336(52)	−0.00332 ^[b]	
Λ_{JK}	μHz	−2.75(31)	−2.48(60)		
Λ_{KKJ}	mHz	0.0278(25)			
Lines		266	194	67	1622
RMS error	kHz	13.3	19.8	13.5	$7.5 \times 10^{-4} \text{ cm}^{-1}$
σ		0.97	0.98	1.01	1.00

Notes: Numbers in parenthesis are one standard deviation and apply to the last significant digits. **[a]** From Ref. [4]. **[b]** Fixed to ground state value.

6. Acknowledgement

This study was supported by Bologna University (RFO funds), MIUR (Project PRIN 2015: STARS in the CAOS, Grant Number 2015F59J3R), and Ca’ Foscari University, Venice (AdiR funds).

References

- [1] M. Sarwar Alam, J. Hwan Jeong, Thermodynamic properties and critical parameters of HFO-1123 and its binary blends with HFC-32 and HFC-134a using molecular simulations, *Int. J. Refrig.* 104 (2019) 311–320.
- [2] M. O. McLinden, J. S. Brown, R. Brignoli, A. F. Kazakov, P. A. Domanski, Limited options for low-global-warming-potential refrigerants, *Nat. Commun.* 8 (2017) 14476.
- [3] M. Hashimoto, T. Otsuka, M. Fukushima, H. Okamoto, H. Hayamizu, K. Ueno, R. Akasaka, Development of new low-GWP refrigerants-refrigerant mixtures including HFO-1123, *Sci. Technol. Built En.* 25 (6) (2019) 776–783. [arXiv:https://doi.org/10.1080/23744731.2019.1603779](https://doi.org/10.1080/23744731.2019.1603779), doi:10.1080/23744731.2019.1603779.
- [4] D. Mann, N. Acquista, E. K. Plyler, Vibrational spectra of trifluoroethylene and trifluoroethylene- d_1 , *J. Chem. Phys.* 22 (9) (1954) 1586–1592.
- [5] D. McKean, CH stretching frequencies, bond lengths and strengths in halogenated ethylenes, *Spectrochim. Acta Part A* 31 (9-10) (1975) 1167–1186.

Table 4: Spectroscopic parameters determined for trifluoroethene in the overtone and combination states.

Parameter	Unit	$\nu_9 = 2$	$\nu_{12} = 2$	$\nu_9 = \nu_{12} = 1$
E	cm^{-1}	464	610	537
A	MHz	10582.13248(78)	10730.4962(22)	10656.5591(41)
B	MHz	3868.72306(23)	3885.44476(24)	3877.20485(78)
C	MHz	2833.35089(10)	2844.51620(12)	2839.28342(14)
Δ_J	kHz	0.70320(11)	0.76091(17)	0.72476(77)
Δ_{JK}	kHz	5.8417(18)	9.2032(25)	7.4041(52)
Δ_K	kHz	4.7432(44)	5.794(39)	4.844(57)
δ_J	kHz	0.175477(52)	0.192589(97)	0.18200(36)
δ_K	kHz	3.9355(15)	5.7471(21)	4.7743(26)
Φ_J	mHz	0.2014 ^[a]		0.2014 ^[a]
Φ_{JK}	Hz	0.019974 ^[a]		0.027(11)
Φ_{KJ}	Hz	-0.163(14)		-0.05527 ^[a]
Φ_K	Hz	0.07529 ^[a]		0.07529 ^[a]
ϕ_J	mHz	0.0768 ^[a]		0.0768 ^[a]
ϕ_{JK}	mHz	9.348 ^[a]		9.348 ^[a]
ϕ_K	Hz	0.11635 ^[a]		0.322(201)
Lines		67	25	25
RMS error	kHz	11.5	11.9	11.8
σ		0.96	1.17	0.95

Notes: Numbers in parenthesis are one standard deviation and apply to the last significant digits. The values for the vibrational energy levels (E) were estimated by using the data listed in Table 1 and without considering the anharmonicity constants. [a] Fixed to ground state value.

- [6] H. Jiang, D. Appadoo, E. Robertson, D. McNaughton, A comparison of predicted and experimental vibrational spectra in some small fluorocarbons, *J. Comput. Chem.* 23 (13) (2002) 1220–1225.
- [7] A. Bhaumik, W. Brooks, S. Dass, The microwave spectrum and structure of trifluoro-ethylene, *J. Mol. Struct.* 16 (1) (1973) 29–33.
- [8] R. Wellington Davis, M. Gerry, Centrifugal distortion in trifluoroethylene, *J. Mol. Spectrosc.* 103 (1984) 187–193.
- [9] H. O. Leung, M. D. Marshall, Rotational spectroscopy and molecular structure of 1, 1, 2-trifluoroethylene and the 1, 1, 2-trifluoroethylene-hydrogen fluoride complex, *J. Chem. Phys.* 126 (11) (2007) 114310.
- [10] R. Visinoni, S. Giorgianni, A. Baldacci, S. Ghersetti, The infrared laser spectrum of $\text{CF}_2=\text{CHF}$ near 1360 cm^{-1} : Rovibrational analysis of the ν_3 fundamental, *J. Mol. Spectrosc.* 172 (2) (1995) 456–463.
- [11] R. Visinoni, S. Giorgianni, A. Baldacci, M. Pedrali, S. Ghersetti, High-resolution infrared measurements and analysis of the ν_4 band of $\text{CF}_2=\text{CHF}$, *J. Mol. Spectrosc.* 182 (2) (1997) 371–377.
- [12] R. Visinoni, S. Giorgianni, A. Baldacci, S. Ghersetti, Diode laser spectroscopy of trifluoroethylene in the $8.6\text{-}\mu\text{m}$ region, *J. Mol. Spectrosc.* 190 (2) (1998) 248–261.
- [13] M. Melosso, B. Conversazioni, C. Degli Esposti, L. Dore, E. Cané, F. Tamassia, L. Bizzocchi, The pure rotational spectrum of $^{15}\text{ND}_2$ observed by millimetre and submillimetre-wave spectroscopy, *J. Quant. Spectrosc. Ra.* 222 (2019) 186–189.
- [14] M. Melosso, B. A. McGuire, F. Tamassia, C. Degli Esposti, L. Dore, Astronomical search of vinyl alcohol assisted by submillimeter spectroscopy, *ACS Earth and Space Chemistry* 3 (7) (2019) 1189–1195. doi:10.1021/acsearthspacechem.9b00055.
- [15] L. Bizzocchi, F. Tamassia, J. Laas, B. Giuliano, C. Degli Esposti, L. Dore, M. Melosso, et al., Rotational and high-resolution infrared spectrum of HC_3N : Global ro-vibrational analysis and improved line catalog for astrophysical observations, *Astrophys. J. Suppl. S.* 233 (2017) 11.
- [16] I. E. Gordon, L. S. Rothman, C. Hill, R. V. Kochanov, Y. Tan, P. F. Bernath, M. Birk, et al., The HITRAN2016 molecular spectroscopic database, *J. Quant. Spectrosc. Ra.* 203 (2017) 3–69.
- [17] J. K. Watson, Aspects of quartic and sextic centrifugal effects on rotational energy levels, *Vibrational spectra and structure*

6 (1977) 1–89.

[18] W. Gordy, R. L. Cook, Microwave molecular spectra, Wiley, 1984.

[19] S. J. Borchert, Low-resolution microwave spectroscopy: A new band type, *J. Mol. Spectrosc.* 57 (2) (1975) 312–315.

[20] Z. Kisiel, The millimeter-wave rotational spectrum of chlorobenzene: Analysis of centrifugal distortion and of conditions for oblate-type bandhead formation, *J. Mol. Spectrosc.* 144 (2) (1990) 381–388.

[21] N. Tasinato, A. Pietropolli Charmet, P. Stoppa, ATIRS package: A program suite for the rovibrational analysis of infrared spectra of asymmetric top molecules, *J. Mol. Spectrosc.* 243 (2) (2007) 148–154.

[22] H. M. Pickett, The fitting and prediction of vibration-rotation spectra with spin interactions, *J. Mol. Spectrosc.* 148 (2) (1991) 371–377.

[23] C. Degli Esposti, L. Dore, M. Melosso, K. Kobayashi, C. Fujita, H. Ozeki, Millimeter-wave and submillimeter-wave spectra of aminoacetonitrile in the three lowest vibrational excited states, *Astrophys. J. Suppl. S.* 230 (2) (2017) 26.